DANMARKS OG GRØNLANDS GEOLOGISKE UNDERSØGELSE RAPPORT 2019/17

Provenance based on trace element distribution in zircon Upper Jurassic sandstones, Danish North Sea

Christian Knudsen, Tonny B. Thomsen & Lars Juul Kjærgaard

GEOLOGICAL SURVEY OF DENMARK AND GREENLAND
DANISH MINISTRY OF ENERGY, UTILITIES AND CLIMATE

GEUS

DANMARKS OG GRØNLANDS GEOLOGISKE UNDERSØGELSE RAPPORT 2019/17

Provenance based on trace element distribution in zircon Upper Jurassic sandstones, Danish North Sea

Christian Knudsen, Tonny B. Thomsen & Lars Juul Kjærgaard

Released 31.12.2019

GEOLOGICAL SURVEY OF DENMARK AND GREENLAND
DANISH MINISTRY OF ENERGY, UTILITIES AND CLIMATE

GEUS

Content

Summary

Zircon from the wells Amalie-1A, Svane-1A, Stork-1, Gwen-1, Ibenholt-1, Xana-1x, Gita-1x and Marsvin (3-7/7 in Norway) were analyzed for 23 elements using Laser Ablation ICP-MS at GEUS. The aim of this is to test if analysis of the trace element content in detrital zircon can be used to identify similarities and differences in provenance of the sandy intervals in the wells studied. The data from the well in the Danish North Sea was compared to zircon mineral chemistry data from GEUS' global zircon database using multi-variate statistical tool SiroSOM.

The fingerprint of the material from Ibenholt-1 is distinct from the rest of the samples as it is characterized by consisting of almost exclusively one type of zircons. This is in good accordance with this sample being igneous rock belonging to the ca. 1500 Ma old basement. Zircons with the same geochemical fingerprint are common in most of the samples in the area and exposed basement of this composition could have been one of the sources for the sands in the area.

The geochemical fingerprint of the samples from Gita-1x, Xana-1x, Stork-1, Gwen-1, Amalie-1A and Svane-1A share many features. The number of zircons that it was possible to analyze from Amalie-1A and Svane-1A is very limited, but the compositions are diverse and an origin from a single source such as erosion of a basement high e.g. can be ruled out. The sample from Marsvin (3-7/7 in Norway), contain zircons with the same fingerprint as found in Gita-1x, Xana-1x and Svane 1A but Marsvin lack some characteristic populations that are found in the other samples. This suggest that if the source of sand to Marsvin also supplied material to e.g. Gita-1x, Xana-1x and Svane 1A, additional material was added from other sources.

Introduction

The present project was performed in co-operation with INEOS and licence partners. The study represents a continuation of the provenance study presented in Knudsen *et al.* (2017) and is a part of the studies reported by Dybkjær *et al.* (2019) and Olivarius *et al.* (2019). Olivarius *et al.* (2019) report the results of the provenance work focused on U/Pb dating of detrital zircon, rutile and apatite as well as investigating the K-feldspar Pb/Pb isotope characteristics.

Objectives

The aim of the present study is to analyze the trace element content in detrital zircon and investigate to what extent this can be used to identify similarities and differences in provenance of the sandy intervals in Amalie-1A, Svane-1A, Stork-1, Gwen-1, Ibenholt-1, Xana-1x, Gita-1x and Marsvin (3-7/7 in Norway). These data was compared to existing zircon mineral chemistry data from GEUS' global zircon database.

Background

The overall picture in the samples analyzed in the provenance studies from the North Sea is, that the detrital zircon are dominated by 1750 to 950 Ma ages with minor amounts of Archean and Caledonian zircons. Further, minor detrital zircon age populations correspond to Cadomian and Variscan ages are found (Knudsen *et al.* 2018; Olivarius *et al.* 2019 & Olivarius *et al.* in prep). This is in line with previously descriptions from the Heno Formation (Weibel and Knudsen 2007). The detrital zircon age distribution patterns suggests multiple events involving recycling and homogenization of the sediment has taken place in the North Sea prior to and during the deposition of the Upper Jurassic sands.

The abundance of the mineral zircon is low in the igneous and metamorphic rocks that form the source for sediments, but zircon contain high concentrations of heavy elements such as U, Th and Rare Earth Elements (REE). These elements are concentrated in the residual melts during the crystallization of magma and incorporated in the late-crystallizing zircon. This is because their large ionic radii and high charge make these elements incompatible in many rock-forming silicate minerals.

Zircons ability to incorporate such large amounts of a wide range of heavy elements makes the mineral an exceptionally useful mineral for mineral-chemical studies. Modern micro-beam analytical techniques make it possible to analyze mineral chemical record in zircon with high precision and high spatial resolution from individual zircon grains. In the present study the chemical composition of the zircon grains that was dated as part of the provenance study was also analyzed for 23 elements (U, Th, Pb, P, Ti, Rb, Sr, Zr, La, Ce, Pr, Nd, Sm, Eu, Gd, Tb, Dy, Ho, Er, Tm, Yb, Lu & Hf).

The zircon grain composition is controlled by the liquid/melt composition at the moment of crystallization and by the physical conditions under which the zircon crystalized. Accordingly, the abundance and ratios of the trace elements are characterizing the geological environment where zircon was formed (Hoskin & Ireland 2000; Belousova *et al.* 2002; Wang *et al.* 2012; Grimes *et al.* 2015; Armstrong-Altrin *et al.* 2017).

There is a huge variation of element contents observed in zircon subsamples from the same rock sample or even within a single grain. Such large variation in the concentrations found for most elements in zircon have been explained by a number of reasons, including the presence of micro-inclusions and complex, dynamic reactions at the zircon/melt interface involving cation substitution, diffusion, melt-polymerization and structure generation (Hoskin, 2000). Ultimately, the zircon trace element fingerprint can suggest the nature of magmatic source region of host rocks (i.e., I-, S-, or A-type magmatism; Barbey *et al.* 1995; Barros *et al.* 2010; Belusova *et al.* 2006; Veevers *et al.* 2005). However, tracing the ultimate source/provenance of the sediment is not the scope of this work. The aim here is to use the fingerprint to test if it is possible to differences and similarities in provenance of the sand.

An example of the geochemical differences in zircon is illustrated in Figure 1. Here the distribution of REE is shown normalised to chondrite compostition (Wang *et al.* 2012). The light (weight) REE are located to the left in the diagram (e.g. La) and the heavy REE to the right (e.g. Yb or Lu). Zircon is generally enriched in heavy REE relative to the light REE and the slope of the curve can be expressed by e.g. by the La/Yb ratio, which is one characteristic of the different geological environments. There is in general a positive anomaly (peak) or relative enrichment in Ce relative to neighboring elements La and Nd, called the Ce-anomaly (Figure 1). This is usually interpreted as caused by variable oxygen fugacity in the magma because Ce can also occur with the valence 4+ whereas the other REE usually has the valence 3+. The size of the Ce-anomaly can be expressed by the ratio Ce/(La+Nd). There is another anomaly at the position of Eu. This is generally a “valley” in zircon and the size of this Eu-anomaly can be expressed by the ratio Eu/(Sm+Gd). This Eu anomaly is also depending on the oxygen fugacity and crystallization history of the magma and characterize different geological environments.

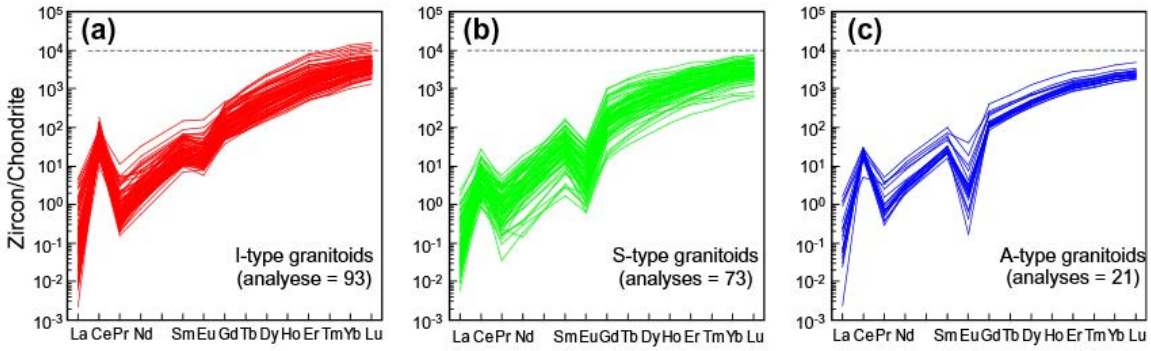

Figure 1 *Chondrite normalized REE patterns for zircons from I-, S- and A-type granitoids (Wang et al. 2012).*

Methods

Analytical methods

Chemical analysis of zircon were performed by laser ablation inductively coupled plasma mass spectrometry (LA-ICPMS) at GEUS, using a NWR 213 laser ablation instrument that is coupled to an Element2 magnetic sector-field ICPMS. The samples were crushed and sieved to extract grains from the 45–750 µm heavy mineral concentrate fraction that was obtained through density separation using a Holman-Wilfley water-shaking table. Zircon grains were then handpicked under binoculars, embedded in epoxy mounts, polished and imaged by cathodoluminescense (CL) using a scanning electron microscopy (SEM) prior to LA-ICPMS analysis.

To minimize instrumental drift, a standard-sample-standard analysis protocol was followed, bracketing all analyses by measurement of the zircon standard GJ-1 (Jackson *et al*. 2004) for the age dating and by the NIST-612 glass reference material for the trace element measurements. For quality control of the trace element analyses, the NIST 614 and the above-mentioned mineral standards were used, typically showing averaged elemental accuracies and precisions within 5 to 10% (2σ) deviation for concentrations above 0.7 ppm.

The trace element and geochronology data were acquired simultaneously from single spots of 25 µm in size, using a laser fluence of ~10 J/cm^2 and a pulse rate of 10 Hz for the zircons and rutiles, and ~9 J/cm^2 and 5 Hz for the apatite analyses. To remove additional Pb contamination, the rutiles were pre-ablated using a 40 µm spot size just prior to analyzing. Total acquisition time for single analyses was max. 2 minutes and included 30–40 sec. background measurement followed by laser ablation for 30 or 40 sec. and washout for 40–45 sec. Factory-supplied software from Thermo-Fisher Scientific was used for the data acquisition, obtained through automated running mode of pre-set analytical spot locations. The analyses spots were set at inclusion-free locations free of cracks on the grains.

Data reduction was performed offline through the Iolite software (Hellström et al., 2008; Paton et al., 2011) using the Iolite-integral VizualAge data reduction scheme (Petrus and Kamber, 2012) for the age dating and the Trace_Elements_IS routine for the elemental determination. Probability-density plots (PDP) combined with histograms were produced through the software jAgeDisplay (Thomsen et al., 2016). Any Tera-Wasserburg, Concordia or age-deriving diagram is produced through Isoplot v.4.15 or Iolite v.2.5. For the PDP, $^{207}Pb/^{206}Pb$ ages were used for zircons older than 700 million years (Ma), whereas $^{206}Pb/^{238}U$ ages were used for younger zircons, as the $^{206}Pb/^{238}U$ ages showed more robust ages and lower uncertainties (2σ) below 700 Ma. To a subset of the analyses from the Ibenholt-1 sample, common-lead correction was applied using measured mass 204 (i.e. ^{204}Hg + ^{204}Pb) corrected for Hg through the $^{202}Hg/^{204}Hg$ natural abundance ratio.

The SiroSOM method

SiroSOM is a data analysis tool that uses the Self-Organising Map (SOM) technique that group data which exhibit common characteristics based on Kohonen's self-organizing map (SOM) algorithm (Kohonen 1981). It is a data-driven analytical approach, which is more objective than more supervised knowledge-driven modelling (a "light version" of machine-learning). In this study we used the commercially available SOM algorithm software application (CSIRO® Self Organizing Maps aka SiroSOM™).

We ran the entire dataset consisting of the 23 elements analysed in all the zircon grains from Ibenholt-1, Gwen-1 (two samples at 4264 and 4245 m respectively), Amalie-1A, Svane-1A, Stork-1, Marsvin, Gita-1x and Xana-1x together with detrital zircon compositions from a large number of heavy mineral deposits in Eastern United States, South and West Africa as well as East, Central and West Australia. The total number of grains used in this analysis is 2586. The aim of this multivariate statistical experiment was to identify the natural compositional groups representing the different geological environments where zircon was formed.

The data was post processed using a procedure developed at GEUS using Matlab to generate plot of the individual samples from the North Sea containing between 26 individual zircon grains (Amalie-1A) and 300 individual zircon grains (Gita-1X).

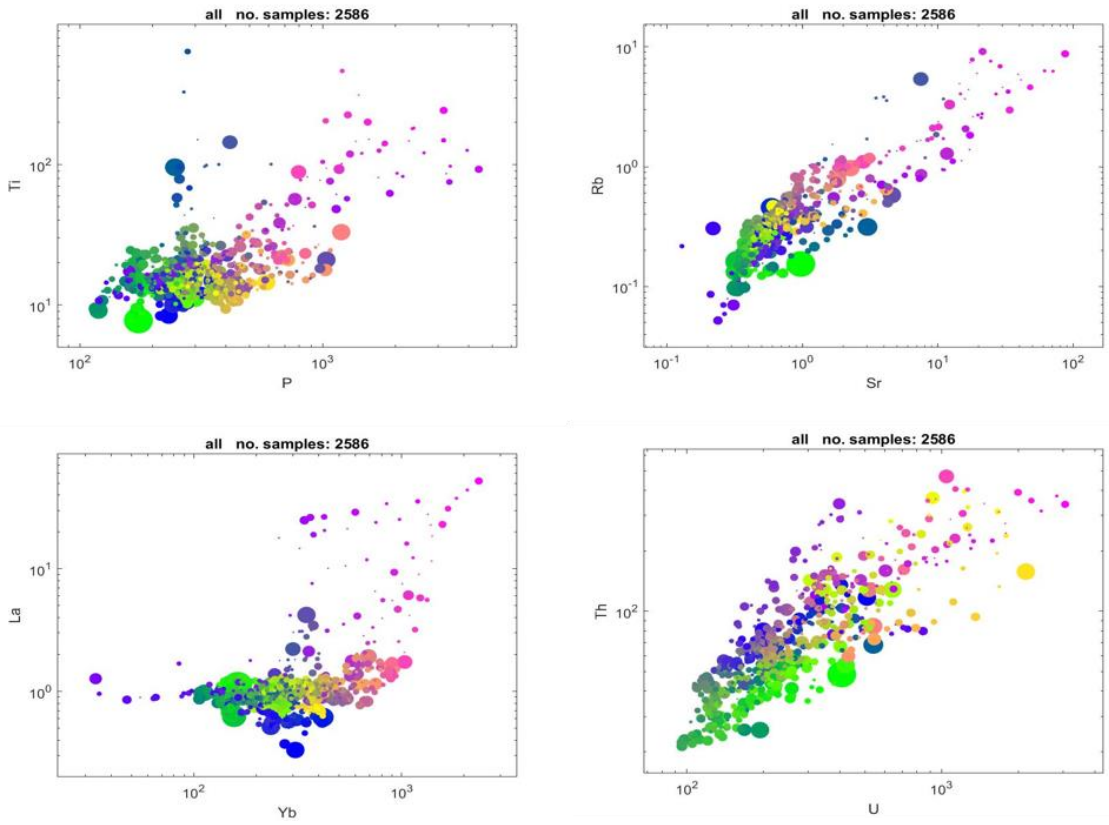

Figure 2 *SiroSOM plot of Ti versus P, Rb versus Sr, La versus Yb and Th versus U. The figure represent the global zircon compositional distribution (incl. the samples from the North Sea) totalling 2586 grains.*

The patterns seen (Figure 2 & 3) are a in this context fingerprinting of the populations to identify similarities and differences. We intend to combine this analysis by adding zircons from known geological environments at a later stage. However, to facilitate the interpretation of the patterns it can be mentioned that:

- The content of Ti in zircon does to some extent reflect the temperature of formation of zircon. (Wark & Watson 2006), and the high Ti blue-green zircons may come from a high temperature environment.
- La and Yb are light and heavy REE respectively and the ratio between these two elements (Figure 2) is an expression of the slope of the REE pattern.
- The ratio between (Sm+Gd) to Eu is an expression of the Eu-anomaly – often depleted relative to Sm and Gd. and it is seen that the different compositional groups (colours) plot in distinctly different fields.
- The ratio between (La+Nd) to Ce is an expression of the Ce-anomaly and zircons generally have enriched Ce values relative to La and Nd. High Ce contents in zircon may imply oxidizing conditions (Ce^{4+} is more compatible than Ce^{3+}).

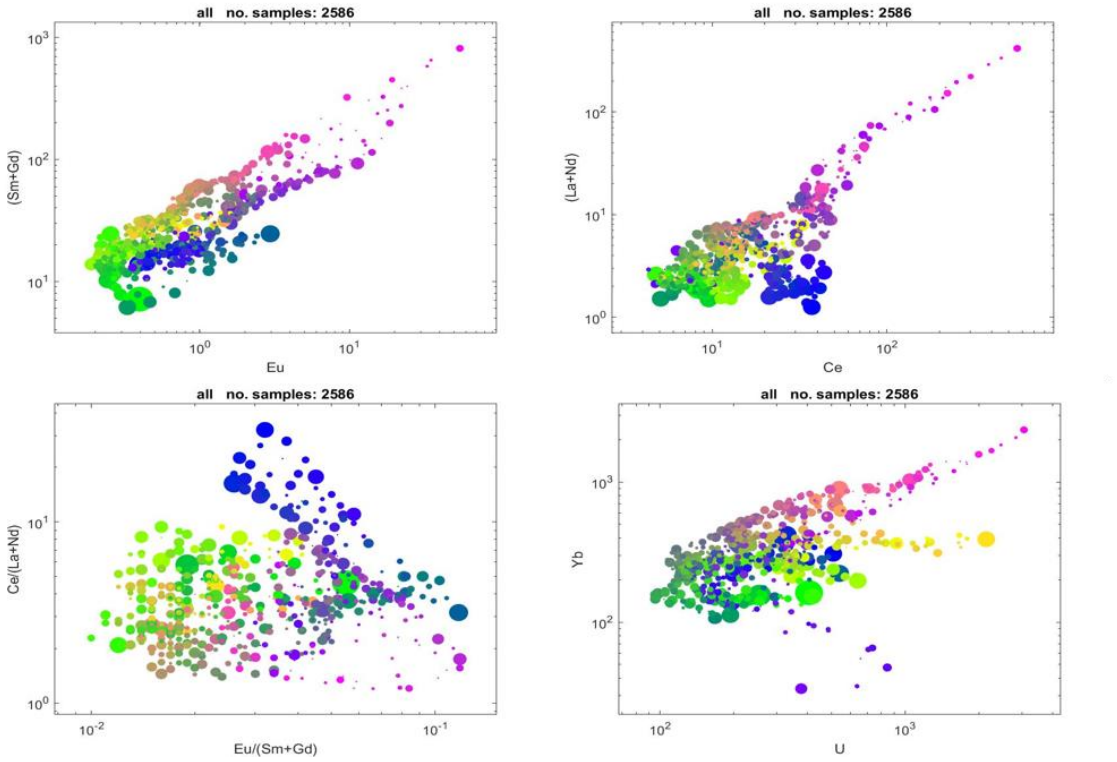

Figure 3 *SiroSOM plot of Sm+Gd versus Eu, La+Nd versus Ce, Ce/(La+Nd) versus Eu/(Sm+Gd) and Yb versus U in all samples.*

The size of the dots represent the number of analyses with the same characteristics falling in the same area – the larger the more analyses in the same area. This way of representation is chosen to avoid dots with different colours on top of each other.

It is emphasised, that the use of the SiroSOM analysis to provenance data is novel.

Results

The results from analysis of the chemical composition of zircons from Amalie-1A, Svane-1A, Stork-1, Gwen-1, Ibenholt-1, Xana-1x, Gita-1x and Marsvin is shown on Figure 4 to 11 using the same SiroSOM chemical classification as shown in Figure 2 and 3. On Figure 4 it is seen that the zircons from Ibenholt-1 have a rather uniform composition in the pink range of colours in contrast to all the other wells that have much more complex compositional distributions.

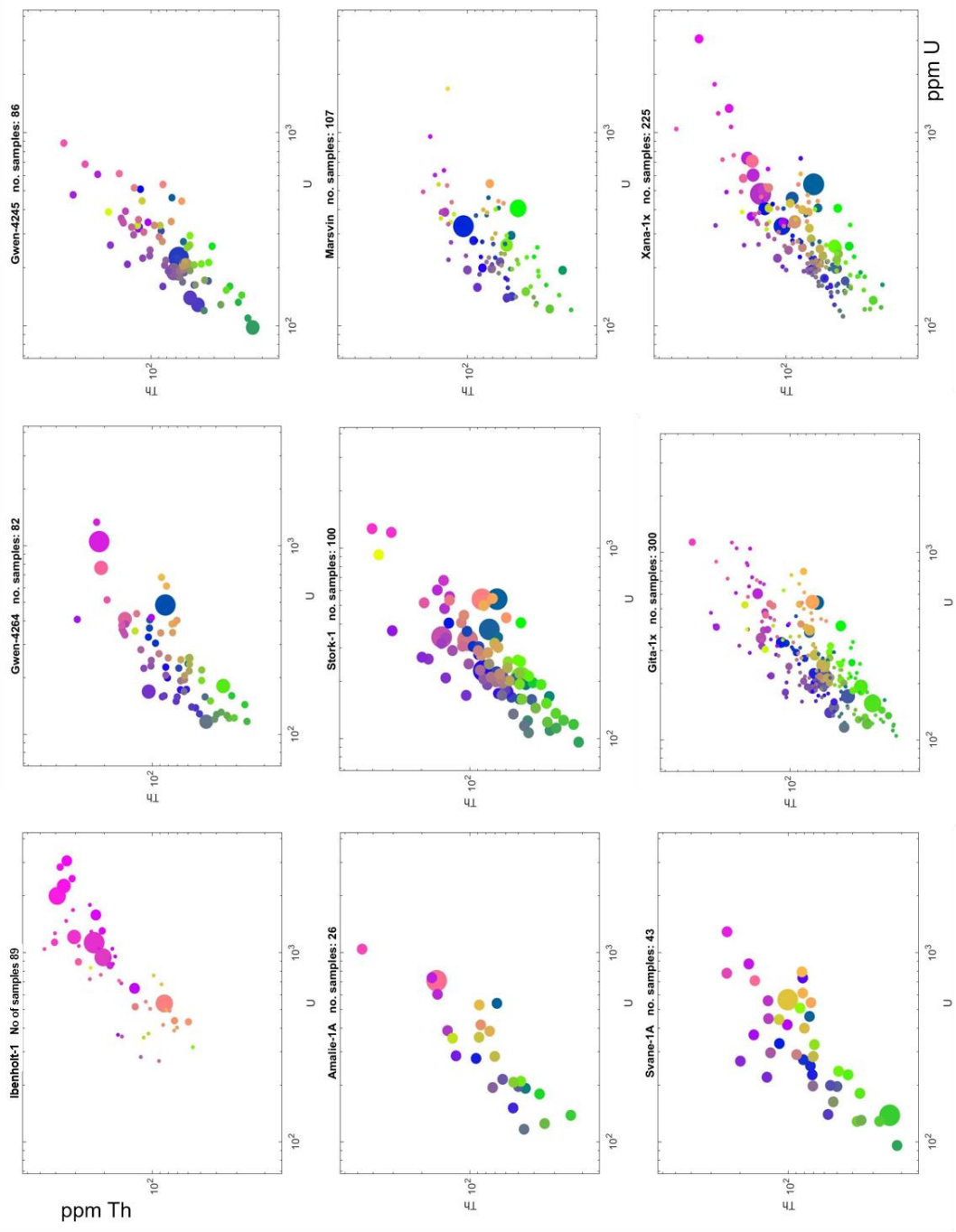

Figure 4 *ppm Th versus ppm U in zircons from the 8 wells investigated.*

The sample from Ibenholt-1 is an igneous rock from the basement explaining why the compositional range is limited. The content of both U and Th is high in most of the zircons from Ibenholt-1 (> 100 ppm Th and > 800 ppm U). These zircons are distinctive.

Zircons from Gita-1x and Zana-1x contain a similar range of compositions. The number of zircons analysed from Svane-1A and Amalie-1A is much lower, but the range of compositions seems to be much the same as in Xana-1x and Gita-1x as well as in Stork-1. An example is the population of light blue zircons (high Ti and low P on Figure 2 and 5) present here but e.g. not present in Marsvin.

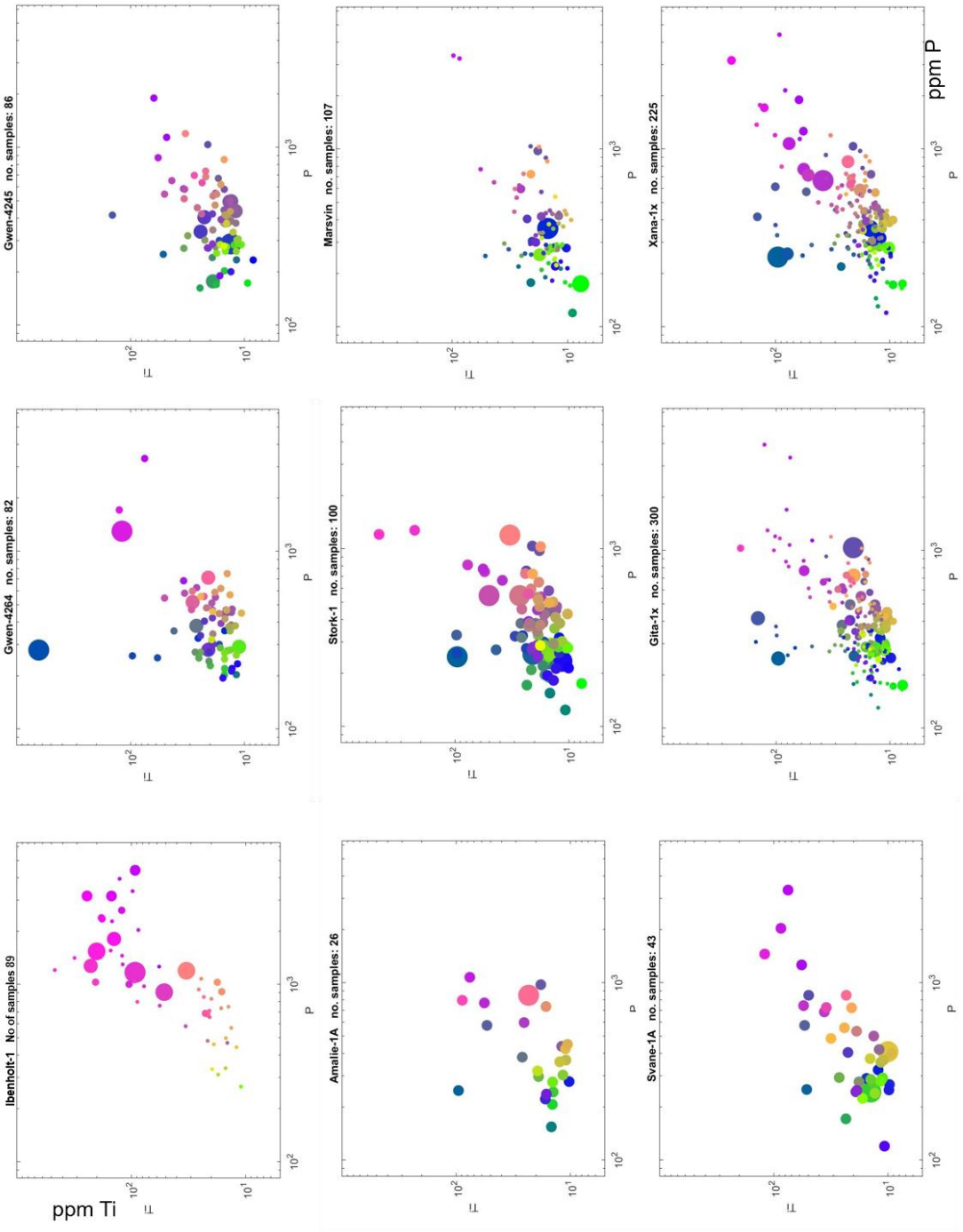

Figure 5 *ppm Ti versus ppm P in zircons from the 8 wells investigated.*

On Figure 6 it can be noted that there is a small population of zircons (blue) characterized by high Rb and Sr present in Svane-1A, Amalie-1A, Xana-1x, Gita-1x as well as in Stork-1 but not in Marsvin and rare in Gwen. Ibenholt-1 has high Rb and Sr.

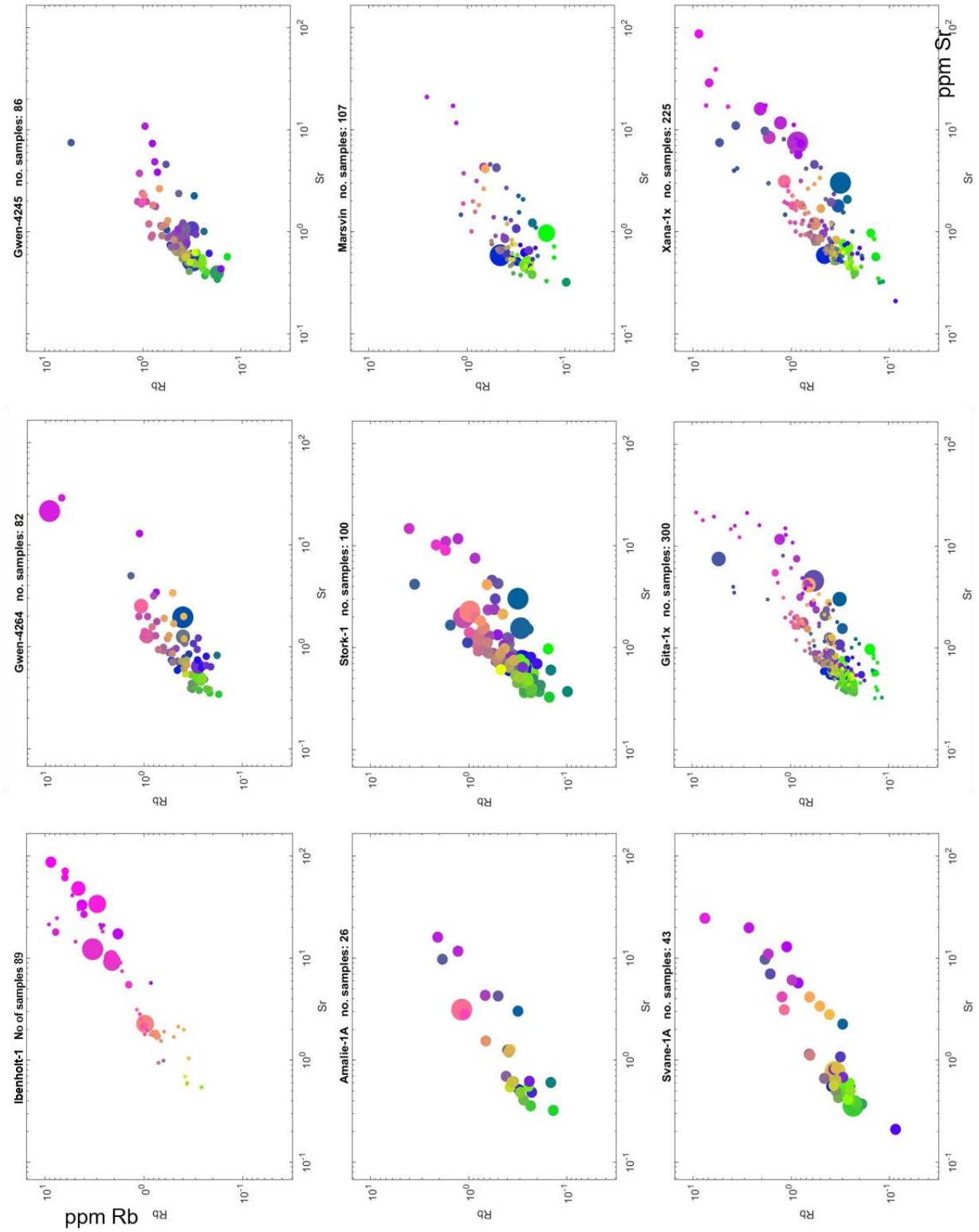

Figure 6 *ppm Rb versus ppm Sr in zircons from the 8 wells investigated.*

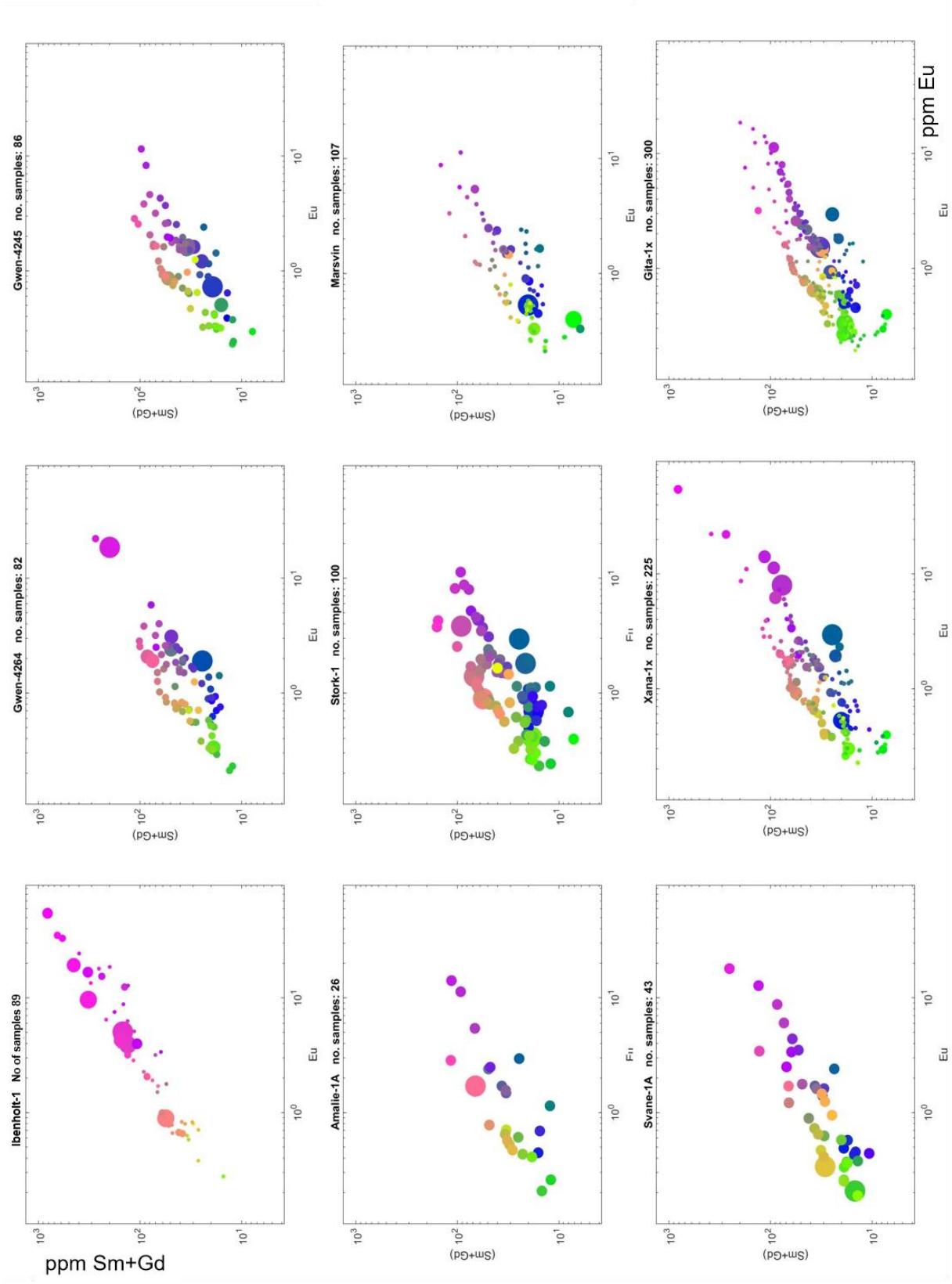

Figure 7 *ppm Sm+Gd versus ppm Eu in zircons from the 8 wells investigated.*

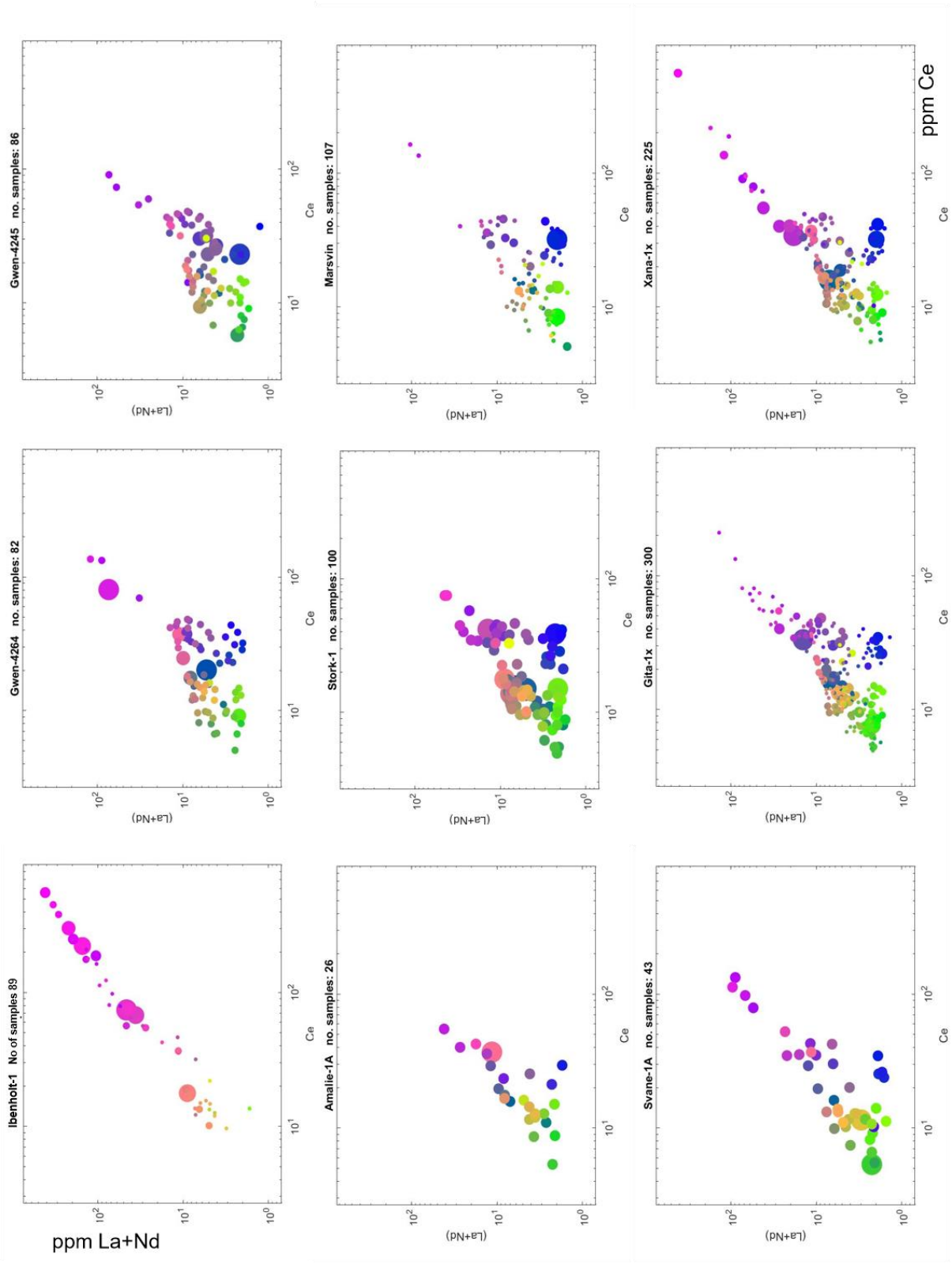

Figure 8 *ppm La+Nd versus ppm Ce in zircons from the 8 wells investigated.*

Gita-1x and Xana-1x as well as Svane-1A contain abundant zircons with high La and Yb (dark pink) where Marsvin only has very few of these zircons (Figure 9).

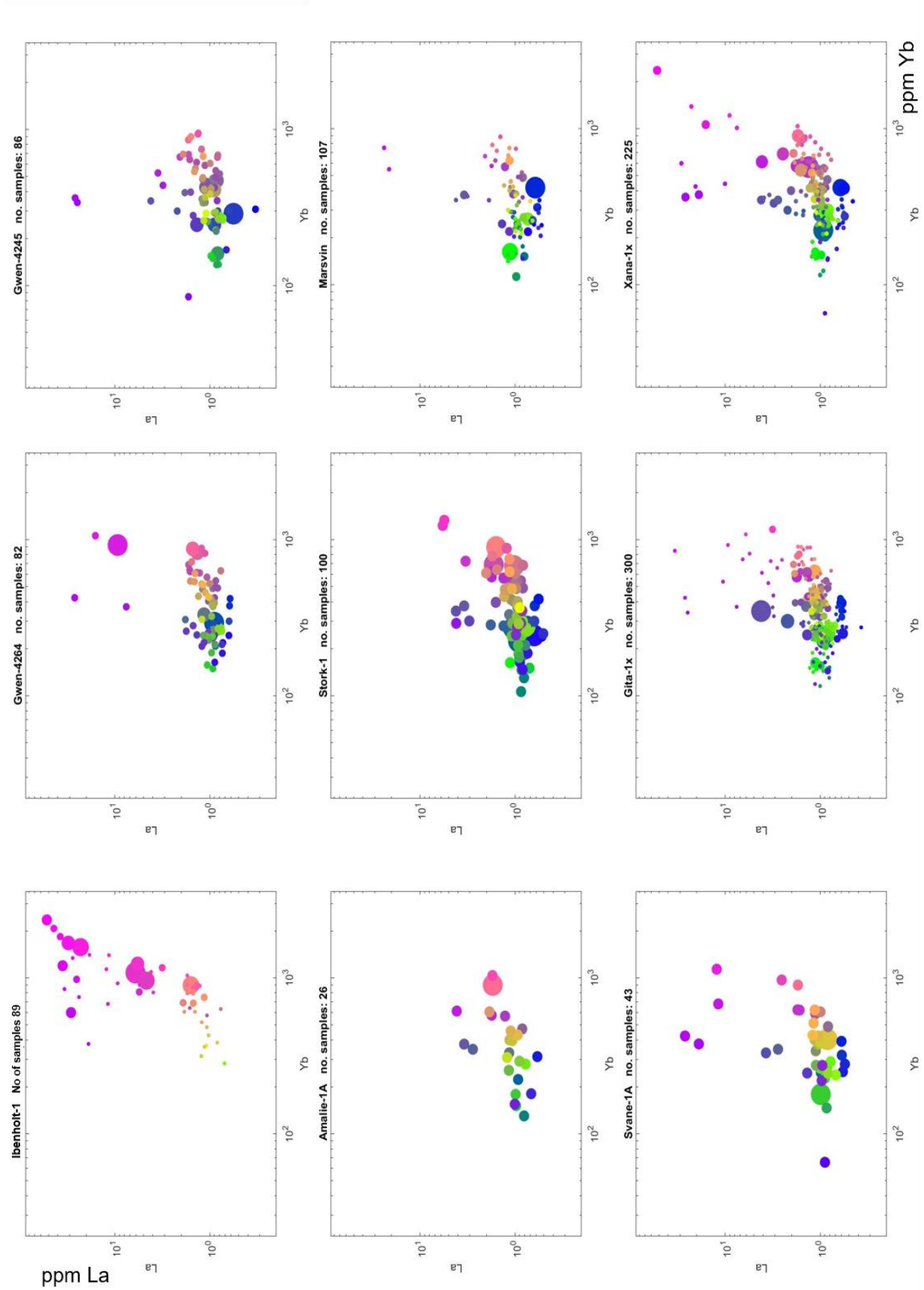

Figure 9 *ppm La versus ppm Yb in zircons from the 8 wells investigated.*

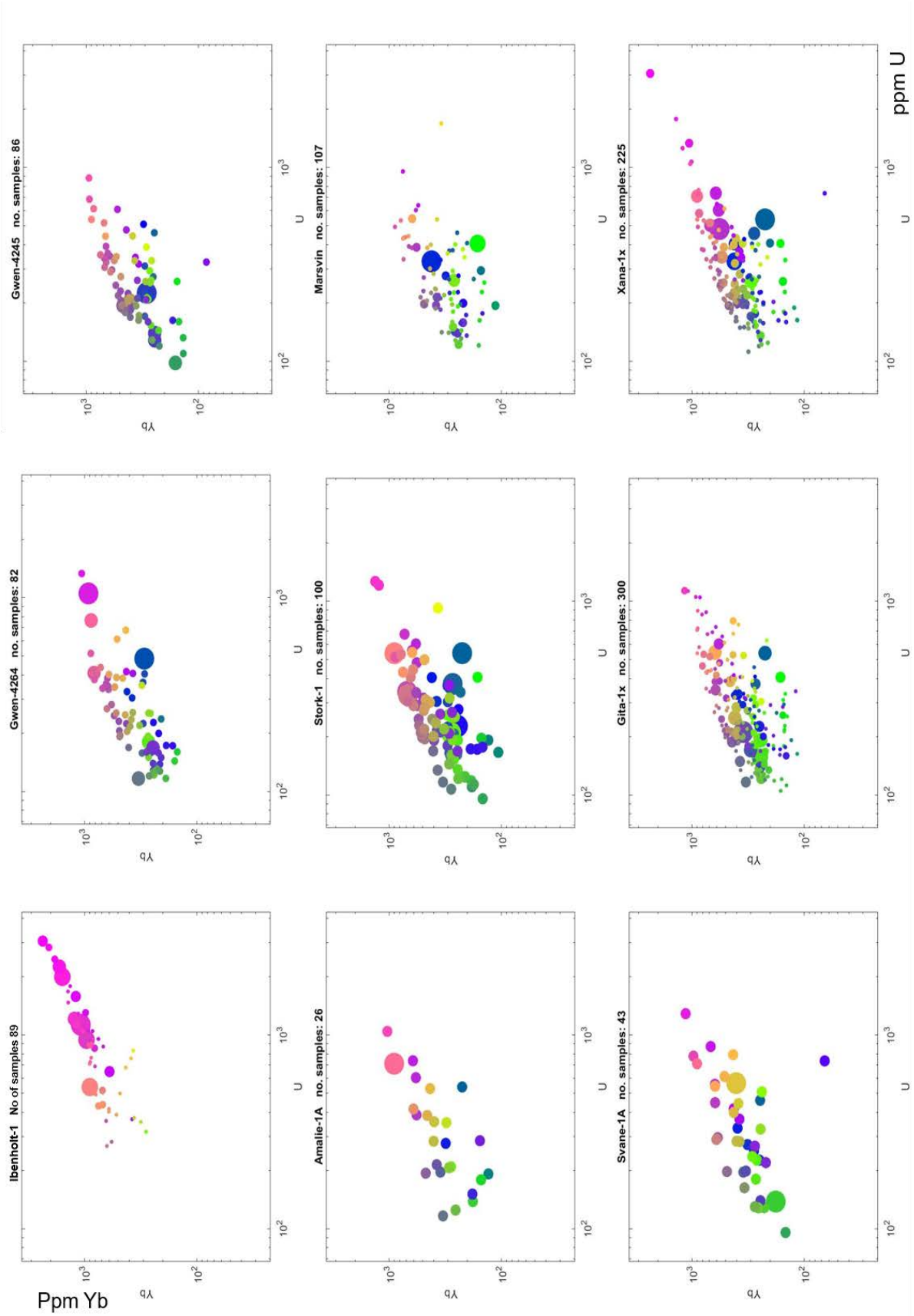

Figure 10 *ppm Yb versus ppm U in zircons from the 8 wells investigated.*

On a plot of the ratios representing the Eu and Ce anomalies in zircon (Figure 11) the difference between Gita-1x, Xana-1x, Stork-1, Amalie-1A and Svane-1A on the one hand and Marsvin on the other can be seen e.g. by the presence of high Eu anomaly and low Ce anomaly (dark pink).

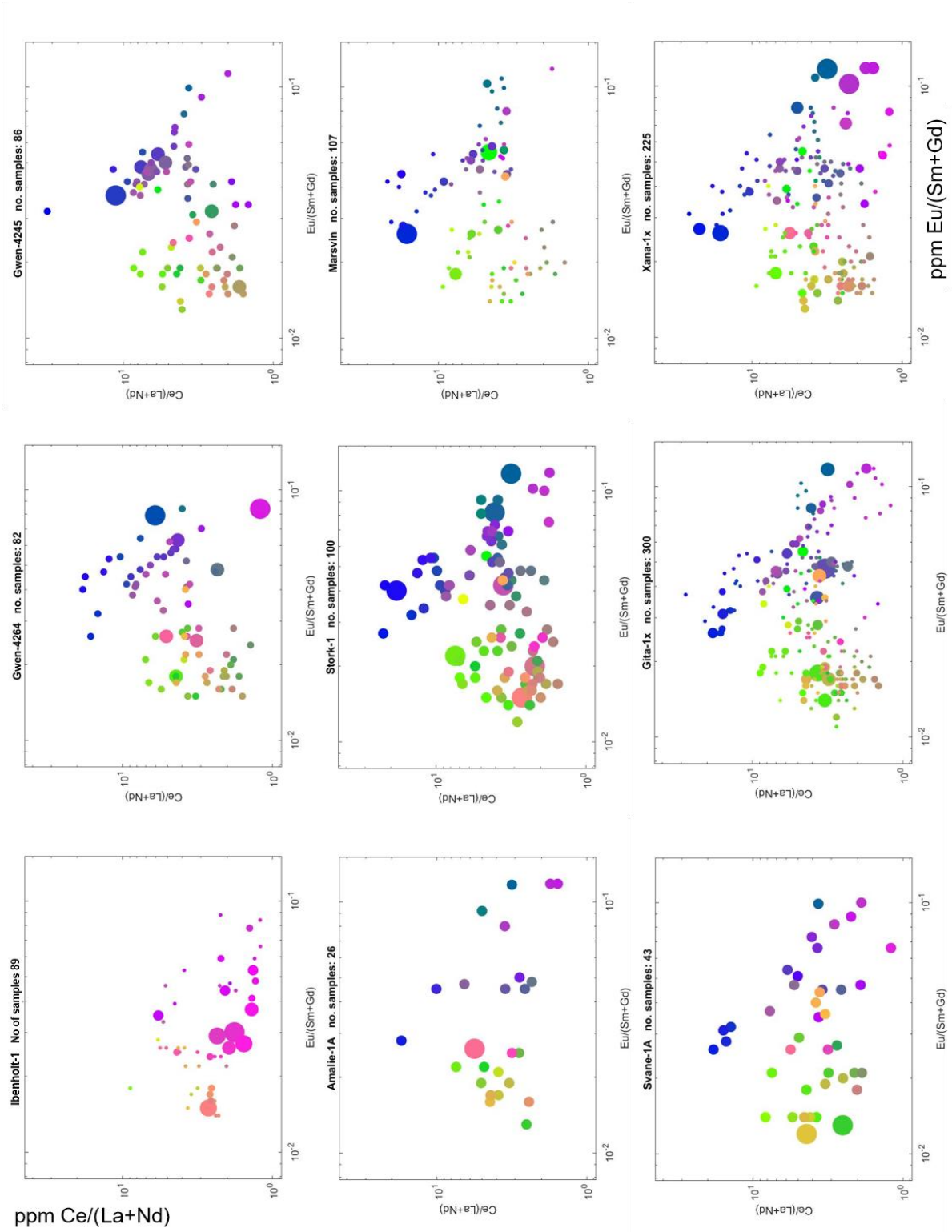

Figure 11 *ppm Yb versus ppm U in zircons from the 8 wells investigated.*

Discussion

The detrital zircon U/Pb age spectra in the Upper Jurassic sandstones in the Danish North Sea suggests that considerable reworking and homogenisation of the sand has taken place. The aim of this study is to test to which extent mineral chemistry in zircon can facilitate interpretations of the sediment distribution during the Upper Jurassic in the Danish North Sea.

The aim is to analyze the zircon fingerprints, to compare these to a global database of zircon chemical compositions and classify the different compositions using SiroSOM. This again to enable visualization of similarities and differences between the provenance of the sandstones in the Upper Jurassic sands in the North Sea.

The fingerprint of the material from Ibenholt-1 is distinct from the rest of the samples as it is characterized by consisting of almost exclusively one type of zircons. This is in good accordance with this sample being igneous rock belonging to the ca. 1500 Ma old basement. Zircons with the same geochemical fingerprint are common in most of the samples in the area, and exposed basement of this composition could have been a source for the sands in the area.

The geochemical fingerprint of the samples from between Gita-1x, Xana-1x, Stork-1, Amalie-1A and Svane-1A share many features. Unfortunately, the number of zircons from Amalie-1A and Svane-1A is very limited, but the compositions are diverse and an origin from a single source such as erosion of a basement high e.g. like the rock exposed in Ibenholt-1 can be ruled out. The sample from Marsvin (3-7/7 in Norway), contain many zircons with the same fingerprint as found in Gita-1x, Xana-1x and Svane 1A but Marsvin lack some characteristic populations that are found in the other samples. This suggest that if the source of sand to Marsvin also supplied material to Gita-1x, Xana-1x and Svane 1A, additional material was added from other sources. The Figures 4 to 11 suggests that the composition of this/those sources could be represented by the dark pink and greenish-blue coloured populations.

The obvious next step could be to compare the groups that was found to compositions of well known geological environments. Further, analysis of the age of the different compositional groups could also serve to constrain the provenance of the zircon populations.

References:

Barbey, P., Allé, P., Brouand, M., Albarède, F., 1995. Rare-earth patterns in zircon from the Manaslu granite and Tibetan Slab migmatites (Himalaya): insights in the origin and evolution of crustally-derived granite magma. Chemical Geology 125, 1–17.

Barros, C.E., Nardi, L.V.S., Dillenburg, S.R., Ayup, R., Jarvis, K., Baitelli, R., 2010. Detrital minerals of modern beach sediments in southern Brazil: a provenance study based on chemistry of zircon. Journal of Coastal Research 26, 80–93.

Belousova, E.A., Grifffin, W.L., O'Reilly, S.Y., Fisher, N.I., 2002. Igneous zircon: trace element composition as an indicator on source rock type. Contributions to Mineralogyand Petrology 143, 602–622.

Belousova, E.A., Griffin, W.L., O'Reilly, S.Y., 2006. Zircon morphology, trace element signatures and Hf-isotope composition as a tool for petrogenetic modeling: examplesfrom eastern Australian granitoids. Journal of Petrology 47, 329–353.

Dybkjær, K., Jakobsen, F.C., Andersen, C., Bjerager, M., Fyhn, M.B.W., Knudsen, C., Knutz, P., Bojesen-Koefoed, J., Kristensen, L., Lauridsen, B.W., Lindström, S., Mørk, F., Nielsen, M.T., Nytoft, H.P., Olivarius, M., Schovsbo, N.H., Weibel, R., 2018. Evaluation of the hydrocarbon exploration potential in the Tail End Graben including the Upper Jurassic Svane and Xana discoveries. Geological Survey of Denmark and Greenland report 2018/48, 25 pp.

Dybkjær, K., Jakobsen, F.C., Andersen, C., Bjerager, M., Fyhn, M.B.W., Knudsen, C., Knutz, P., Bojesen-Koefoed, J., Kristensen, L., Lauridsen, B.W., Lindström, S., Mørk, F., Nielsen, M.T., Nytoft, H.P., Olivarius, M., Schovsbo, N.H., Weibel, R., 2019: XXX. Geological Survey of Denmark and Greenland report 2019/xx.

Hanchar, J.M., Westrenen, W., 2007. Rare earth element behavior in zircon-meltsystems. Elements 3, 37–42.

Liz, J.D., Nardi, L.V.S., Lima, E.F., Jarvis, K., 2009. Geochemistry of trace elements in zircon from the Lavras do Sul Shoshonitic Association, southernmost Brazil. The Canadian Mineralogist 47, 833–846.

Hellström, J., Paton, C., Woodhead, J., Hergt, J., 2008. Iolite: Software for spatially re-solved LA- (quad and MC) ICPMS analysis. In: Sylvester, P. (Ed.) Laser ablation ICP–MS in the earth sciences: current practices and outstanding issues. Mineral. Assoc. of Canada, Quebec, 343–348.

Hoskin, P.W.O., Schaltegger, U., 2003. The composition of zircon and igneous and metamorphic petrogenesis. Reviews in Mineralogy and Geochemistry 53, 27–62.

Kohonen, T. 1981: Automatic formation of topological maps of patterns in a self-organizing system. In: Oja, E. & Simula, O. (eds) Proc. 2SCIA, Scand. Conf. on Image Analysis, Helsinki, Finland. Suomen Hahmontunnistustutkimuksen Seura r. y., 214−220.

Knudsen, C., Weibel, R., Serre, S.H., Thomsen, T., 2017. Provenance investigations related to the Xana-1 well. Zircon and rutile provenance in Xana-1, Gita-1, Amalie-1, Svane-1 and Marsvin-1. Geological Survey of Denmark and Greenland report 2017/50, 17 pp.

Olivarius, M., Knudsen, C., Thomsen, T.B., Serre, S., Jakobsen, & Dybkjær, K. 2019: Provenance data of Upper Jurassic sandstones in the greater Tail End Graben area. Geological Survey of Denmark and Greenland report 2019/13. 18 pp.

Olivarius, M., Knudsen, C., Weibel, R., Lahaye, Y., Thomsen, T.B., Serre, S., Jakobsen, F., Bjerager, M., Mørk, F. & Dybkjær, K. In Prep: Combined K-feldspar, zircon, rutile and apatite provenance interpretation, Upper Jurassic sandstones, Danish North Sea.

Paton, C., Hellstrom, J. C., Paul, P., Woodhead, J. D. & Hergt, J.M. 2011: Iolite: Freeware for the visualisation and processing of mass spectrometric data. Journal of Analytical Atomic Spectrometry 26, 2508-2518.

Petrus, J. A, & Kamber, B. S. 2011: VisualAge: A novel approach to U-Pb LA-ICP-MS geochronology. Goldschmidt Conference Abstracts, Mineralogical Magazine, 1633.

Veevers, J.J., Saeed, A., Belousova, E.A., Griffin, W.L., 2005. U-Pb ages and source composition by Hf-isotope and trace element analysis of detrital zircons in Permian sandstone and modern sand from southwestern Australia and a review of the paleogeographical and denudational history of the Yilgarn Craton. Earth-ScienceReviews 68, 245–279.

Wang, Q., Zhu, D. C., Zhao, Z. D., Guan, Q., Zhang, X. Q., Sui, Q. L., Hu, Z-C. & Mo, X. X. 2012: Magmatic zircons from I-, S-and A-type granitoids in Tibet: trace element characteristics and their application to detrital zircon provenance study. Journal of Asian Earth Sciences, 53, 59-66.

Wark, D. A., & Watson, E. B. 2006: TitaniQ: a titanium-in-quartz geothermometer. Contributions to Mineralogy and Petrology, 152, 743-754.

Weibel, R. & Knudsen, C. 2007: Chemostratigraphy and mineral chemical fingerprinting: Heno Formation, Danish North Sea. Danmarks og Grønlands Geologiske Undersøgelse Rapport 2007/42. 165 pp.